

Simulation of Non-metallic Inclusion Deposition and Clogging of Nozzle

Hadi Barati, Menghuai Wu, Tobias Holzmann, Abdellah Kharicha and Andreas Ludwig

Abstract Motion of non-metallic inclusions (NMIs) in molten steel and deposition of them on nozzle wall leading to clogging are simulated using a two-way coupling model. In this model different steps of clogging have been considered including transport of NMIs by turbulent melt flow towards the nozzle wall, adhesion of the NMI on the wall, and formation and growth of clogging material by the NMI deposition. The model is used to simulate clogging in a pilot scale device. The results show that the model reproduces these clogging steps well until complete blockage of the flow path in the nozzle. It is found that clog growth step plays critical role for prediction of the clogging process and understanding melt flow and NMI behaviors during the process. Without implementation of this step, unrealistic melt flow rate is obtained leading to incorrect particle deposition rate. In addition, if the clog growth is ignored, distribution of deposition material becomes more uniform with overestimated amount of total deposition mass.

Keywords Clogging · Non-metallic inclusion · Deposition · Nozzle
Steel casting

H. Barati · M. Wu · T. Holzmann (✉) · A. Kharicha · A. Ludwig
Chair for Modeling and Simulation of Metallurgical Processes, Department of Metallurgy,
Montanuniversitaet Leoben, Franz-Josef Street 18, 8700 Leoben, Austria
e-mail: tobias.holzmann@unileoben.ac.at

H. Barati
e-mail: hadi.barati@unileoben.ac.at

M. Wu
e-mail: menghuai.wu@unileoben.ac.at

H. Barati
K1-MET, Franz-Josef Street 18, 8700 Leoben, Austria

Introduction

Blockage of submerged entry nozzle (SEN) is a long-term problem in steel continuous casting. It can result in operation disruptions and different casting defects [1–3]. Among several mechanisms suggested for clogging, deposition of non-metallic inclusions (NMIs) as de-oxidation and re-oxidation products, e.g. Al_2O_3 , on the SEN wall is considered as the primary reason [4], because similar morphologies and chemical compositions of NMIs were observed in the melt, clog material, and as-cast product [5].

Clogging generally occurs through four steps, as depicted in Fig. 1: (1) transport of particles to the wall, (2) interactions of the fluid and the particles with the wall, (3) formation and growth of the clog, and (4) probable fragmentation or resuspension of the clog.

High temperature, opaque nature of steel melt, and difficulties of precise control of steel casting make experimental investigation of the process very hard. Therefore, numerical modeling provides a helpful tool to study the clogging process. Diverse modeling efforts have been made for the clogging of SEN by emphasizing one or more critical steps of Fig. 1. Bai and Thomas [6] studied the effect of the clog on the flow through a slide-gate nozzle and Zhang et al. [1] investigated influence of blocking half of one out-port of the SEN. They manually changed the geometry of SEN to mimic the as build clog. To model clogging the Eulerian-Lagrangian approach is a common method which provides detailed information about particle and its trajectory. It was used to find correlations between SEN designs and clogging tendency [7], to study the influence of the velocity gradient of the melt flow and the turbulent kinetic energy on the particle deposition [8], and to investigate effects of SEN diameter on clogging [9]. Eulerian-Eulerian is also used to simulate the inclusion deposition rate in a SEN [10, 11].

Most of the modeling efforts about SEN clogging focused only on the fluid flow and particle transport, i.e. step 1 of Fig. 1, and other steps were ignored. Moreover,

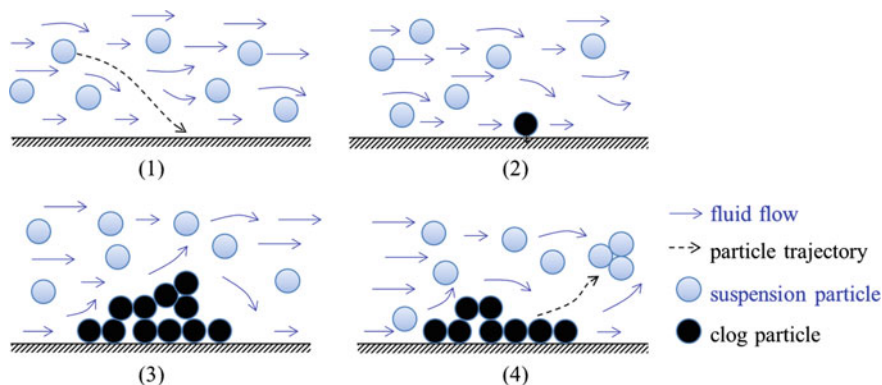


Fig. 1 Schematic of clogging phenomenon (four steps)

in previous simulations clogging was assumed as a steady process and SEN wall stays clean during the process. To the knowledge of authors, none of them has calculated mutual interactions of the clog growth with the melt flow. In the current paper a transient model has been proposed to simulate nozzle clogging in pilot scale by considering the further clogging step (steps 1–3). The current version of the model neglects fragmentation of the clog (step 4).

Model in Brief

In the present paper an Eulerian-Lagrangian model as developed by the authors [12] is used. The flow of the melt as the primary continuous medium is described by the conservation equations of mass and momentum. To model the turbulence, shear-stress transport (SST) k - ω model is adopted. The solid non-metallic inclusions are assumed as spherical particles and a force balance of buoyancy, drag, lift, virtual mass, and pressure gradient controls motion of them. The equations for the turbulent flow and forces acting on particle are listed in Tables 1 and 2, respectively.

Due to the different structure of flow in bulk and near the wall, a stochastic model [13], which is developed for particle motion in wall-bounded flow, is used for wall boundary cells.

Table 1 Governing equations for the fluid flow

Conservation equations	Symbol definition
Mass	$\nabla \cdot (\rho \vec{u}) = 0$
Momentum	$\rho \frac{\partial \vec{u}}{\partial t} + \nabla \cdot (\rho \vec{u} \vec{u}) = -\nabla p + \nabla \cdot (\mu \nabla \cdot \vec{u}) + \vec{S}_u$
Turbulence kinetic energy	$\rho \frac{\partial k}{\partial t} + \nabla \cdot (\rho k \vec{u}) = \nabla \cdot (\Gamma_k \nabla \cdot k) + \tilde{G}_k - Y_k + S_k$
Specific dissipation rate	$\rho \frac{\partial \omega}{\partial t} + \nabla \cdot (\rho \omega \vec{u}) = \nabla \cdot (\Gamma_\omega \nabla \cdot \omega) + G_\omega - Y_\omega + D_\omega + S_\omega$

ρ : density of fluid (kg/m³)
 μ : viscosity of fluid (kg m⁻¹ s⁻¹)
 t : time (s)
 \vec{u} : velocity of fluid (m/s)
 k : turbulence kinetic energy (m² s⁻²)
 ω : specific dissipation rate of turbulence kinetic energy (s⁻¹)
 Γ_k, Γ_ω : diffusivity for k and ω (kg m⁻¹ s⁻¹, kg m⁻²)
 \tilde{G}_k, G_ω : generation of turbulence kinetic energy for k and ω (kg m⁻¹ s⁻³, kg m⁻² s⁻²)
 Y_k, Y_ω : dissipation of k and ω (kg m⁻¹ s⁻³, kg m⁻² s⁻²)
 D_ω : cross-diffusion term of ω (kg m⁻² s⁻²)
 S_k, S_ω, \vec{S}_u : source term due to porous medium of clog (kg m⁻¹ s⁻³, kg m⁻² s⁻², kg m⁻² s⁻²)

Table 2 Equations for particle transport and forces acting on a particle in bulk flow

Equation	Symbols definition	
Particle transport	$m_p \frac{d\vec{u}_p}{dt} = \vec{F}_B + \vec{F}_D + \vec{F}_L + \vec{F}_{VM} + \vec{F}_{press}$	\vec{u}_p : velocity of particle (m/s)
Buoyancy force	$\vec{F}_B = \frac{(\rho_p - \rho) \pi d_p^3}{6} \vec{g}$	m_p : mass of particle (kg)
Drag force	$\vec{F}_D = \frac{1}{8} \pi d_p^2 \rho C_D \vec{u} - \vec{u}_p (\vec{u} - \vec{u}_p)$ $C_D = \begin{cases} \frac{24}{Re_p}, & \text{if } Re_p \leq 0.1 \\ \frac{24}{Re_p} (1 + 0.15 Re_p^{0.687}), & \text{if } 0.1 \leq Re_p \leq 10^3 \\ 0.44, & \text{if } Re_p > 10^3 \end{cases}$ $Re_p = \frac{ \vec{u} - \vec{u}_p d_p \rho}{\mu}$	\vec{g} : gravity (m s ⁻²) ρ_p : density of particle (kg m ⁻³) d_p : diameter of particle (m) C_D : drag coefficient (-) Re_p : particle Reynolds number (-)
Lift force	$\vec{F}_L = -\frac{9}{4\pi} \mu d_p^2 U_s \text{sgn}(G) \left(\frac{\rho}{\mu} G \right)^{\frac{1}{2}} \vec{J}$	U_s : difference between instantaneous streamwise velocities for fluid and particle (m s ⁻¹)
Virtual mass force	$\vec{F}_{VM} = \frac{\rho \pi d_p^3}{12} \frac{d}{dt} (\vec{u} - \vec{u}_p)$	G : local velocity gradients (s ⁻¹)
Pressure gradient force	$\vec{F}_{press} = \frac{\rho \pi d_p^3}{6} \frac{D\vec{u}}{Dt}$	J : correction factor of the lift force (-)

When a NMI meets the SEN wall, made of refractory or ceramic, the capillary force, also termed adhesion force, is the dominant force. Several studies concluded that once the capillary force is imposed, the particle stays in contact with the wall [14–16]. The model has considered a tricking probability of particles as they approaching wall. This sticking probability must be determined experimentally or using other models. In this paper, it is assumed to be 100%. To couple particle deposition with the fluid flow pattern, two stages are considered for clogging. In early stage, particle deposition leads to change in wall roughness, as shown in Fig. 2a, b. This stage lasts until the roughness height is larger than half of boundary cell thickness. Thereafter, in later stage, the computational cell is converted to a porous medium, marked in gray in Fig. 2c. Further deposition results in fully occupation of the cell by particles, as indicated by line pattern in Fig. 2d. Neighbor cells then are exposed to particle deposition. Hence, the clog material grows as a porous medium. Regarding to the permeability of the clog, Darcy source terms are applied for the clog region to take into account the effects of clog growth on the fluid flow. More details about the model can be found in [12].

Clogging in a pilot scale device which has been used to investigate the nozzle clogging [1, 17, 18] has been simulated. This device is made from a laboratory induction furnace and a circular nozzle with 5 mm diameter as situated at the bottom of the furnace. Molten steel flows through the nozzle until clogging in the nozzle stops the flow. Figure 3 shows mesh and boundary conditions. Regarding the physics controlling the process, multiphase fluid flow (melt and air) is modeled

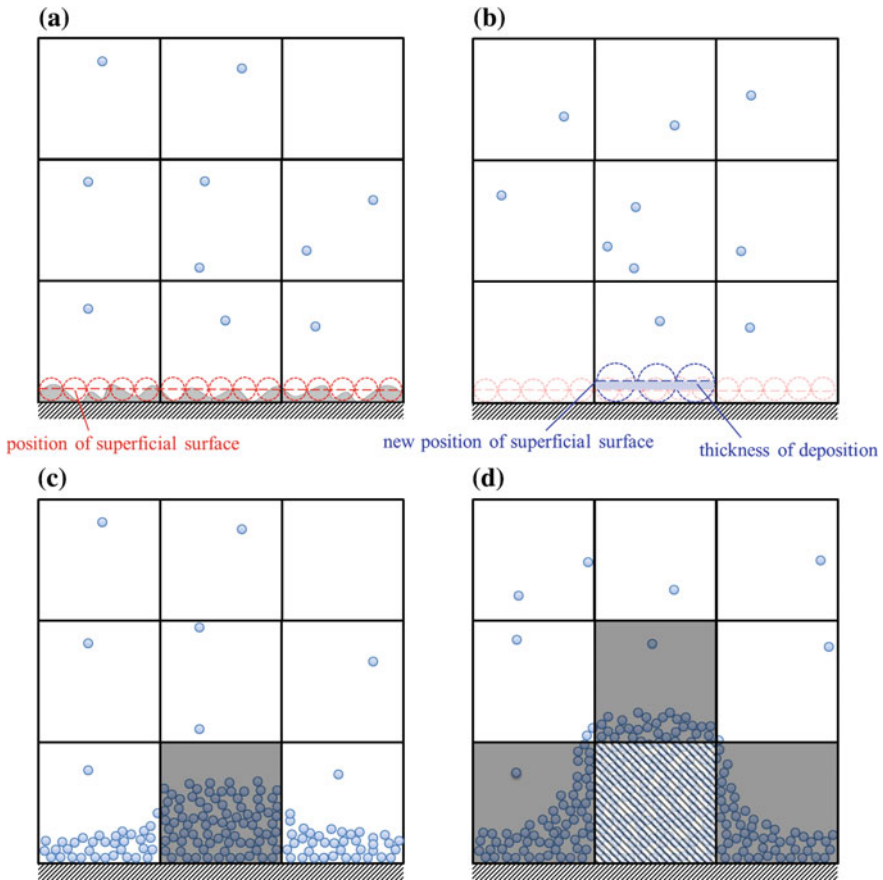


Fig. 2 Schematic illustration of clogging evolution in the model: **a** initial wall roughness considered as uniform sand-grain roughness, **b** enhanced wall roughness due to the particle deposition, **c** formation of porous clog, and **d** clog growth

using volume of fluid (VOF) method. On the top surface, pressure-inlet boundary condition is set for air, and for the nozzle outlet, pressure-outlet is imposed. Due to the gravity, the furnace becomes empty gradually. However, due to the clogging, the nozzle could be blocked before run out of the whole melt. Non-slip boundary condition is applied on all walls. To save computation costs and avoid unimportant calculation of particle tracking in the furnace, particles are injected on the connection plane between bottom of the furnace and top of the nozzle. A full 3D domain is simulated and the equations are numerically solved using commercial CFD code ANSYS-FLUENT with extended user defined functions (UDFs) for considering the growth of clog.

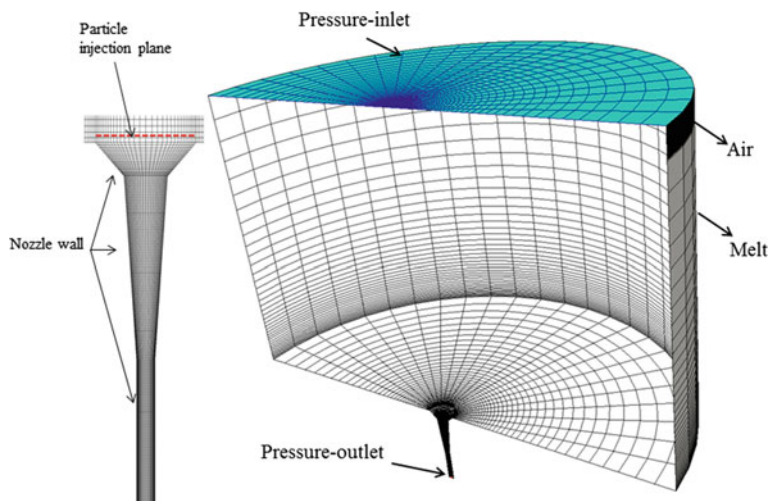


Fig. 3 Computational domain and boundary conditions. The initial interface between air and melt is plotted on the furnace wall

Results and Discussion

Clogging process and the clog growth are plotted in Fig. 4 by snapshots of the clog from different views. It shows that after 50 s a smooth layer of deposited material covers the nozzle wall. Continuous deposition of particles leads to formation of some bulges in narrowest section of the nozzle and a part of the middle section. Growth of the clog bulges finally blocks the flow passage as shown at 250 s.

In Fig. 5a velocity magnitude during the process is plotted on a vertical symmetry plane. The clog front is marked by solid lines and here the velocity magnitude in the clog material decreases because of its porous character. At 250 s the melt still flows due the small hole left in the clog, as shown in Fig. 4, however the value of the melt velocity is negligible. Figure 5b depicts a zoomed view of the flow field and the clog at 150 s. It shows how the presence of the clog changes the flow pattern. Some eddies can be found below bulges which may result in trapping of particles and finally attaching them to the clog. Therefore, it reveals that two-way coupling between flow field and particle deposition is critical to understand the clogging process.

To show the importance of clog growth in simulation of clogging, particle deposition results are compared with a case without effects of clog growth on the melt flow, i.e. particles are deleted from calculation once reach the nozzle wall and nozzle wall stays with constant roughness during the process. In Fig. 6 total deposition mass along height of the nozzle is shown for different times. The comparison of two graphs indicates that in both cases at first, deposition is almost uniform and then after 100 s becomes wavy. In the case (a) deposition mass decreases dramatically at $y = 0.040$ m when $t = 200$ s, while it happens at $y = 0.054$ m fore case (b).

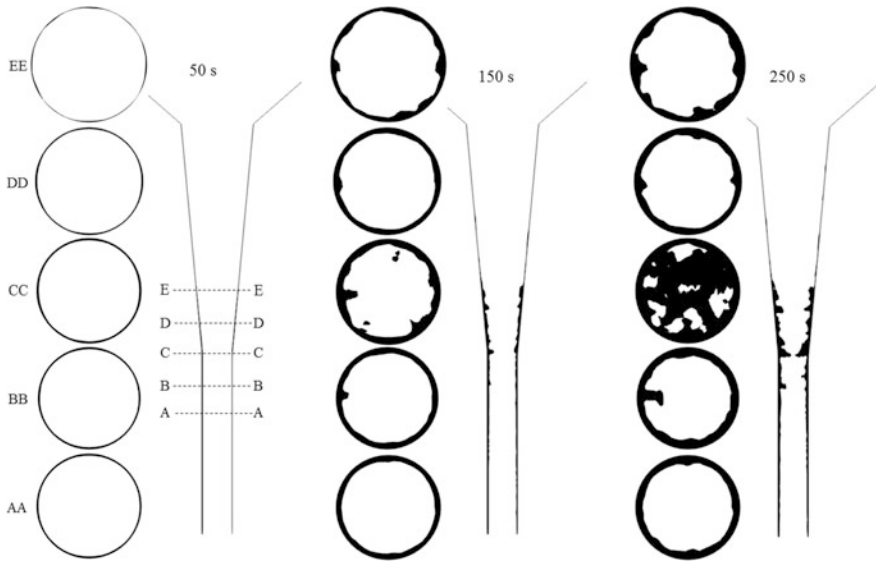


Fig. 4 Evolution of the clogging in the nozzle. Horizontal cross sections in different heights and the vertical sections are shown at different times

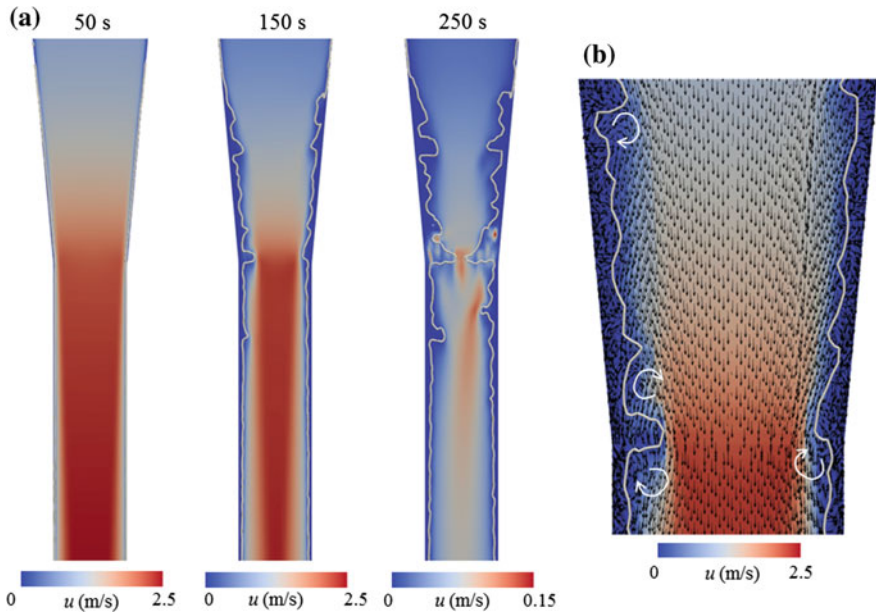


Fig. 5 Changes in melt velocity magnitude during clogging process (a) and zoomed view of flow arrows at 150 s (b). The clog front is marked by solid lines

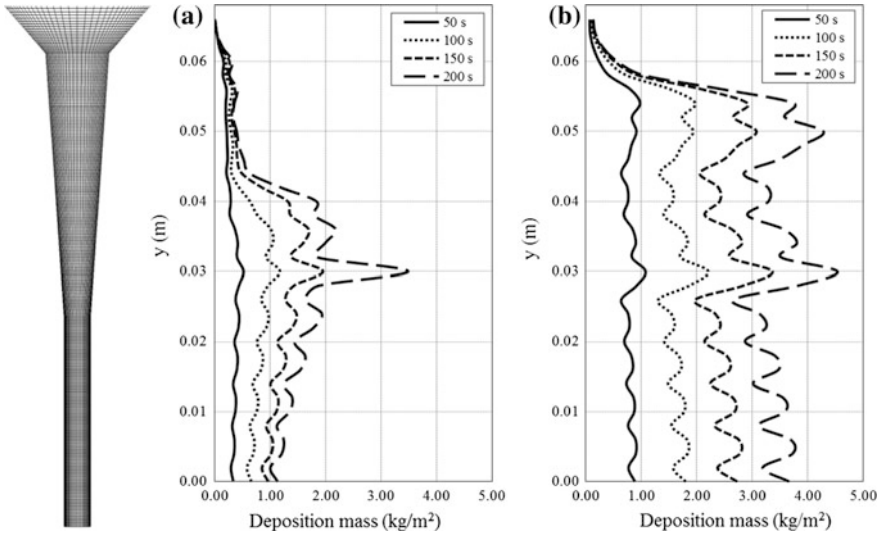
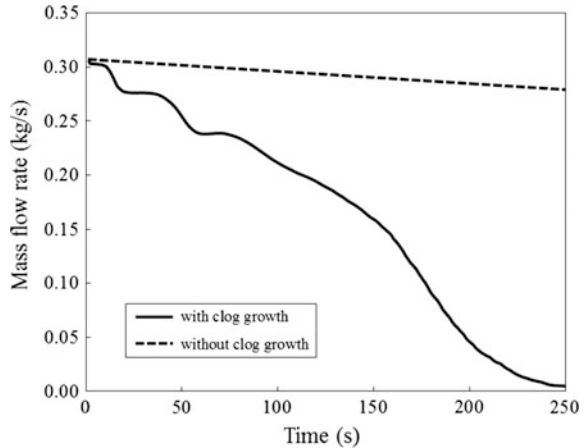


Fig. 6 Comparison of deposition mass along nozzle height during time with (a) and without (b) considering the clog growth

Moreover, the maximum deposition occurs at $y = 0.03$ m in case (a), whereas in case (b), maximum deposition happens at $y = 0.03$ and 0.05 m. The difference between deposition mass at maximum peak(s) and other positions in Fig. 6a is much larger than that in Fig. 6b. However without clog growth, case (a), initial deposition areas can be found, they may change after a while due to the change of the flow pattern, as found in case (b). The deposition mass values generally in Fig. 6b are larger than those in Fig. 6a. It is because of different melt flow rates in two cases, as shown in Fig. 7. In case (a), the melt flow rate decreases during the process because

Fig. 7 Mass flow rate of the melt during the process with and without considering the clog growth



of narrowing of the flow passage in addition to hydrostatic pressure loss. While, in case (b), the only reason is the hydrostatic pressure loss. Therefore, simulation without considering clog growth leads to unrealistic results and would show incorrect time and region of nozzle blockage.

Conclusions

A two-way coupling model is used to simulate clogging in pilot scale. The model covers most of clogging steps, i.e. transport of particles by turbulent flow, deposition of particle on the wall, and growth of the clog due to the particle deposition. Interactions between particle deposition and fluid flow are taken into account in two stages: enhancement of wall roughness in early stage of particle deposition and development of clog as a porous medium in later stage. The simulation results declare that the model can reproduce clogging steps well particularly clog growth step. This step is critical to understand the clogging as a transient process. In the present pilot scale neglecting the clog growth leads to unrealistic high melt flow rate and hence incorrect particle deposition rate for whole process. Moreover, when the clog growth is ignored, distribution of deposition material on the nozzle is modeled much more uniform than that when the clog growth is considered in the simulation.

Acknowledgements The research leading to these results has received funding from the European Union's Research Fund for Coal and Steel (RFGS) research program under grant agreement No. RFSR-CT-2014-00009. The authors also gratefully acknowledge the funding support of K1-MET, metallurgical competence center. The research program of the K1-MET competence center is supported by COMET (Competence Center for Excellent Technologies), the Austrian program for competence centers. COMET is funded by the Federal Ministry for Transport, Innovation and Technology, the Federal Ministry for Science, Research and Economy, the provinces of Upper Austria, Tyrol and Styria as well as the Styrian Business Promotion Agency (SFG).

References

1. Zhang L, Wang Y, Zuo X (2008) Flow transport and inclusion motion in steel continuous-casting mold under submerged entry nozzle clogging condition. *Metall Mater Trans B* 39(4):534–550
2. Vermeulen Y, Coletti B, Blanpain B, Wollants P, Vleugels J (2002) Material evaluation to prevent nozzle clogging during continuous casting of Al killed steels. *ISIJ Int* 42(11): 1234–1240
3. Kojola N, Ekerot S, Jönsson P (2011) Pilot plant study of clogging rates in low carbon and stainless steel grades. *Ironmak. Steelmak* 38(2):81–89
4. Thomas BG, Bai H (2001) Tundish nozzle clogging-application of computational models. In: *Proceedings of the 18th process technology division conference*, Warrendale, Pennsylvania, 25–28 Mar 2001

5. Singh SN (1974) Mechanism of alumina buildup in tundish nozzles during continuous casting of aluminum-killed steels. *Metall Trans* 5(10):2165–2178
6. Bai H, Thomas BG (2001) Turbulent flow of liquid steel and argon bubbles in slide-gate tundish nozzles: part I. Model development and validation. *Metall Mater Trans B* 32(2): 253–267
7. Sambasivam R (2013) Clogging resistant submerged entry nozzle design through mathematical modelling. *Ironmak Steelmak* 33(6):439–453
8. Mohammadi-Ghaleni M, Zaeem MA, Smith JD, O'Malley R (2016) Comparison of CFD simulations with experimental measurements of nozzle clogging in continuous casting of steels. *Metall Mater Trans B* 47(6):3384–3393
9. Long M, Zuo X, Zhang L, Chen D (2010) Kinetic modeling on nozzle clogging during steel billet continuous casting. *ISIJ Int* 50(5):712–720
10. Ni P, Jonsson LTI, Ersson M, Jönsson PG (2014) The use of an enhanced Eulerian deposition model to investigate nozzle clogging during continuous casting of steel. *Metall Mater Trans B* 45(6):2414–2424
11. Ni P, Jonsson LTI, Ersson M, Jönsson PG (2014) On the deposition of particles in liquid metals onto vertical ceramic walls. *Int J Multiph Flow* 62:152–160
12. Barati H, Wu M, Kharicha A, Ludwig A (2017) A transient model for nozzle clogging—part I: model description. *Powder Technol.* (Manuscript under review)
13. Guingo M, Minier JP (2008) A stochastic model of coherent structures for particle deposition in turbulent flows. *Phys Fluids* 20(5):053303
14. Heuzeroth F, Fritzsche J, Werzner E, Mendes MA, Ray S, Trimis D, Peuker UA (2015) Viscous force—an important parameter for the modeling of deep bed filtration in liquid media. *Powder Technol* 283:190–198
15. Sasai K, Mizukami Y (2001) Mechanism of alumina adhesion to continuous caster nozzle with reoxidation of molten steel. *ISIJ Int* 41(11):1331–1339
16. Uemura KI, Takahashi M, Koyama S, Nitta M (1992) Filtration mechanism of non-metallic inclusions in steel by ceramic loop filter. *ISIJ Int* 32(1):150–156
17. Janis D, Karasev A, Inoue R, Jönsson PG (2015) A study of cluster characteristics in liquid stainless steel and in a clogged nozzle. *Steel Res Int* 86(11):1271–1278
18. Roos E, Karasev A, Jönsson PG (2015) Effect of Si and Ce contents on the nozzle clogging in a REM alloyed stainless steel. *Steel Res Int* 86(11):1279–1288